Interpreting increases in $|S_L|$ due to channel coupling

R. S. Mackintosh*
Department of Physical Sciences, The Open University, Milton Keynes, MK7 6AA, UK
(Received 12 April 2013; revised manuscript received 26 September 2013; published 4 November 2013)

We present various cases where the coupling of breakup or transfer channels to the elastic channel leads to an increase in the elastic channel $|S_L|$ for particular values of L. Particular emphasis is given to ^{6}Li, ^{7}Be, and ^{8}B scattering from ^{58}Ni and ^{6}He scattering from ^{208}Pb, all near the Coulomb barrier. A link is proposed to the fact that ^{8}B has a larger breakup cross section while its elastic scattering angular distribution is less modified by breakup than ^{6}Li and ^{7}Be at the same energy relative to the barrier; an argument is made relating this to non-local processes. We also describe cases of ^{6}He scattering from ^{208}Pb at energies far above the Coulomb barrier, of heavy ion scattering, and of ^{2}H and ^{3}He scattering. The effect is absent in otherwise similar proton scattering cases. The increase in $|S_L|$ is associated with strongly absorptive potentials and excitation processes that keep an excited amplitude of the projectile from the absorptive region prior to de-excitation to the elastic channel. The possible relevance to direct reactions is proposed.

DOI: 10.1103/PhysRevC.88.054603 PACS number(s): 24.50.+g, 24.10.Ht, 24.10.Eq

I. INTRODUCTION

The total reaction cross section σ_R is related to the elastic scattering S matrix S_L through the relation

$$\sigma_R = \sum_L \sigma_L = \frac{\pi}{k^2} \sum_L (2L+1)(1-|S_L|^2), \qquad (1)$$

where $\hbar k$ is the momentum in the center-of-mass (c.m.) system. Since σ_L represents the contribution to the reaction cross section for partial wave L, it is natural to suppose that the coupling of reaction channels to the elastic channel would result in a decrease in $|S_L|$ as a result of flux generated in the reaction channels with the same conserved quantum numbers. In general, this is observed to happen, but there are circumstances where the coupled channels increase $|S_L|$. A specific case was discussed in Ref. [1] where deuteron breakup led to increased $|S_L|$ for certain L and particular energies. It was found that the "wrong way" (WW) effect is correlated with other effects, in particular the occurrence of generative (emissive) regions in the dynamic polarization potential (DPP) generated by the coupling to breakup channels. Such effects are related to the non-locality and L dependence of nucleon-nucleus and nucleus-nucleus interaction potentials. The present paper takes a first step in illuminating this relationship by surveying the various cases that we are aware of where the WW effect has been found. We point out correlates of WW that might contribute to understanding elastic scattering. In this paper, RW (right way) indicates cases where channel coupling reduces $|S_L|$.

In what follows, WW effects will be associated with non-local effects. To be clear, we therefore note that "non-locality" in the context of nuclear scattering often refers to non-locality arising from knock-on exchange; this accounts for most of the energy dependence of the local nucleon optical model potential (OMP). But exchange is not the only source of non-locality, and Feshbach's theory [2] clearly predicts that the nuclear optical potential has dynamically generated non-locality, and also L dependence, and specific calculations [3–5] show this explicitly. Thus, the non-locality of the nuclear optical potential should not be identified exclusively with that arising from exchange, particularly since this will have a short range for composite particles [6]. It will be argued in what follows that dynamical non-local effects for composite projectiles are directly related to WW occurrences. This is important because direct reaction calculations generally involve OMPs that are local and L independent. A rigorous understanding of direct reactions with light ions is obviously desirable, but it is particularly essential for applying direct reactions in, for example, precise studies of nuclei that might undergo neutrinoless double-β decay [7] and for extracting the structure of exotic nuclei [8,9], for example.

The WW effect was noted long ago [10] (though not called that then), but a variety of new examples suggest that understanding WW might throw light on some very general questions concerning the simplest nuclear reaction: elastic scattering. Of course, elastic scattering is not really simple, but it is important since what happens in elastic scattering affects every nuclear reaction in which an optical potential plays a role in the analysis.

The WW effect is particularly evident in the scattering of weakly bound nuclei at energies near the Coulomb barrier, and this is the subject of Sec. II. In Sec. III more diverse examples are discussed and some regularities revealed. Section IV summarizes and discusses the possible implications.

II. SCATTERING AND BREAKUP NEAR THE COULOMB BARRIER

A. Comparing ^{6}Li, ^{7}Be, and ^{8}B on ^{58}Ni

The reactions of ^{6}Li, ^{7}Be, and ^{8}B on ^{58}Ni near the Coulomb barrier have recently been studied by Aguilera *et al.* [11] who present evidence that ^{8}B behaves like a proton-halo nucleus in a way that the other two nuclei do not. Projectile breakup for the same three cases was the subject of continuum discretized coupled channel (CDCC) calculations [12] from

*r.mackintosh@open.ac.uk

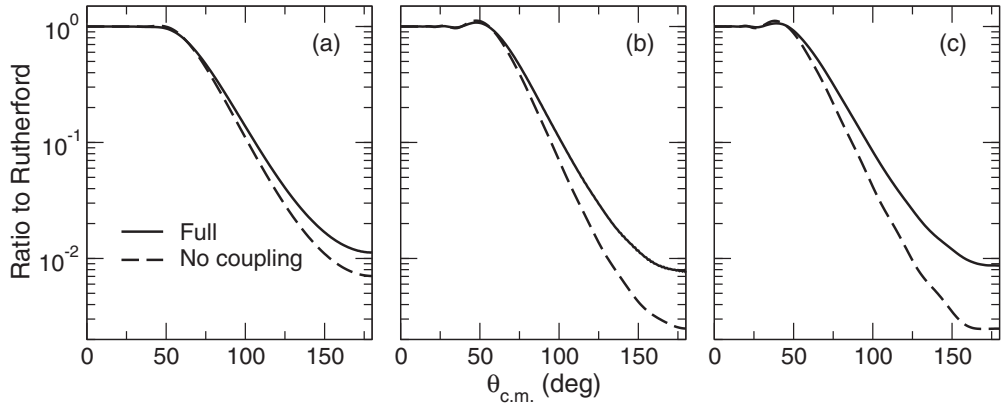

FIG. 1. CDCC calculations for (a) ^{8}B on ^{58}Ni at $E_{\rm lab} = 29.26$ MeV, (b) ^{7}Be on ^{58}Ni at $E_{\rm lab} = 24.12$ MeV, (c) ^{6}Li on ^{58}Ni at $E_{\rm lab} = 19.04$ MeV. Solid and dashed curves denote full and no-coupling results, respectively.

which it emerged that the scattering of ^{8}B was distinctly different from the scattering of ^{6}Li and ^{7}Be in other respects, see also [13]. The association between these effects invites an examination of these cases as a source of possible further understanding of reactions near the barrier, and perhaps more general nuclear reactions. In what follows the emphasis is upon how dynamic processes affect elastic scattering, not upon fusion. It is relevant to what follows that the Coulomb contribution to the breakup (BU) of ^{8}B is greater than for ^{7}Be and much greater than for ^{6}Li. The contribution of Coulomb dipole coupling is very different for the three cases, the relevant factor, see Ref. [14], $(Z_2A_1 - A_2Z_1)/(A_1A_2)$ being 0, 1/6, and 3/7 for ^{6}Li, ^{7}Be, and ^{8}B, respectively. In this expression, Z_n and A_n are the atomic number and mass number of the nth cluster of the projectile.

In Ref. [12], CDCC BU calculations were studied for ^{6}Li at 19.04 MeV, ^{7}Be at 24.12 MeV, and ^{8}B at 29.26 MeV all incident on ^{58}Ni; the energies were adjusted so that each was the same relative to the relevant Coulomb barrier. The following behaviors were found within the two-cluster BU model:

1. As shown in Fig. 1 of [12], adapted here as Fig. 1, projectile breakup (BU) had a relatively small effect on the elastic scattering differential cross section (DCS) for ^{8}B on ^{58}Ni at about 30 MeV, compared to the ^{6}Li and ^{7}Be cases at similar energies relative to the barrier.
2. The breakup (BU) cross section $\sigma_{\rm BU}$ for ^{8}B was relatively large, compared to that for the ^{6}Li and ^{7}Be cases.
3. The WW effect, while considerable for ^{8}B, was less pronounced than it was for the other two cases. This is discussed below.

The apparently paradoxical result (that a larger BU effect was associated with a smaller effect on differential cross section) was reviewed in Ref. [13] where values of the breakup cross sections $\sigma_{\rm BU}$ were presented. In the present paper, we also quote and illustrate some results for ^{6}Li scattering from ^{58}Ni at 24.6 MeV, a somewhat higher energy with respect to the barrier than the other cases.

An alternative characterization of the paradoxical result comes from considering the change in the total cross section, $\Delta\sigma_{\rm R}$, induced by the BU coupling, see Table I. Note that $\sigma_{\rm BU} > \Delta\sigma_{\rm R}$ for each case, implying that BU decreases the aggregate cross section for all other processes, including fusion; this turns out to be usual for breakup reactions, at least within the model. Furthermore, the much smaller change in the angular distribution for ^{8}B elastic scattering than for the other cases corresponds to a much larger change $\Delta\sigma_{\rm R}$ in the total reaction cross section $\sigma_{\rm R}$ than for ^{7}Be. The change in $\sigma_{\rm R}$ for ^{6}Li is of the about the same magnitude but of opposite sign for ^{8}B. The change in elastic scattering angular distribution for ^{8}B is much less than for the other two cases which change in visually similar ways, see Fig. 1. These facts appear to be at odds with the use of fits to elastic scattering to determine reaction cross sections; see, e.g., Ref. [15]. However, there are differences in the angular distribution which are less easy to see from the figures: unlike the other cases, both with and without BU coupling, for ^{8}B there is no peak in the angular distribution just before the rapid Fresnel-like falloff.

The changes in $\sigma_{\rm R}$ are intelligible from the changes in $|S_L|$ shown in Fig. 2 of Ref. [12], adapted here as Fig. 2, when one considers how the quantity $\sum_L (2L+1)(1-|S_L|^2)$ changes, as implied by that figure. For ^{8}B, $|S_L|$ is WW for low L and RW for high L, but high L wins out in the sum through the $2L+1$ weighting, hence the large $\Delta\sigma_{\rm R}$. It is not very clear from Fig. 2, but for ^{7}Be the strong WW for low L is balanced by some degree of RW for high L resulting from long-range Coulomb breakup. There is little such compensating RW for ^{6}Li since there is no long-range dipole BU acting at high L in this case, which is characterized by the strong WW effect for $L \lesssim 12$. Thus, the BU coupling for ^{6}Li leads

TABLE I. For ^{6}Li, ^{7}Be, and ^{8}B scattering from ^{58}Ni, the change in $\sigma_{\rm R}$ due to breakup coupling $\Delta\sigma_{\rm R}$, the breakup cross section $\sigma_{\rm BU}$ and the extent to which the breakup cross section exceeds the increase in reaction cross section, $\sigma_{\rm BU} - \Delta\sigma_{\rm R}$. For ^{7}Be, $\sigma_{\rm BU}$ includes the cross section for the inelastic excitation of the bound $\frac{1}{2}^-$ state (30 mb).

Projectile	$E_{\rm lab}$ (MeV)	$\Delta\sigma_{\rm R}$	$\sigma_{\rm BU}$(mb)	$\sigma_{\rm BU} - \Delta\sigma_{\rm R}$
^{6}Li	19.04	− 73.49	47	120.49
^{7}Be	24.12	8.59	51	42.41
^{8}B	29.26	85.31	130	44.69

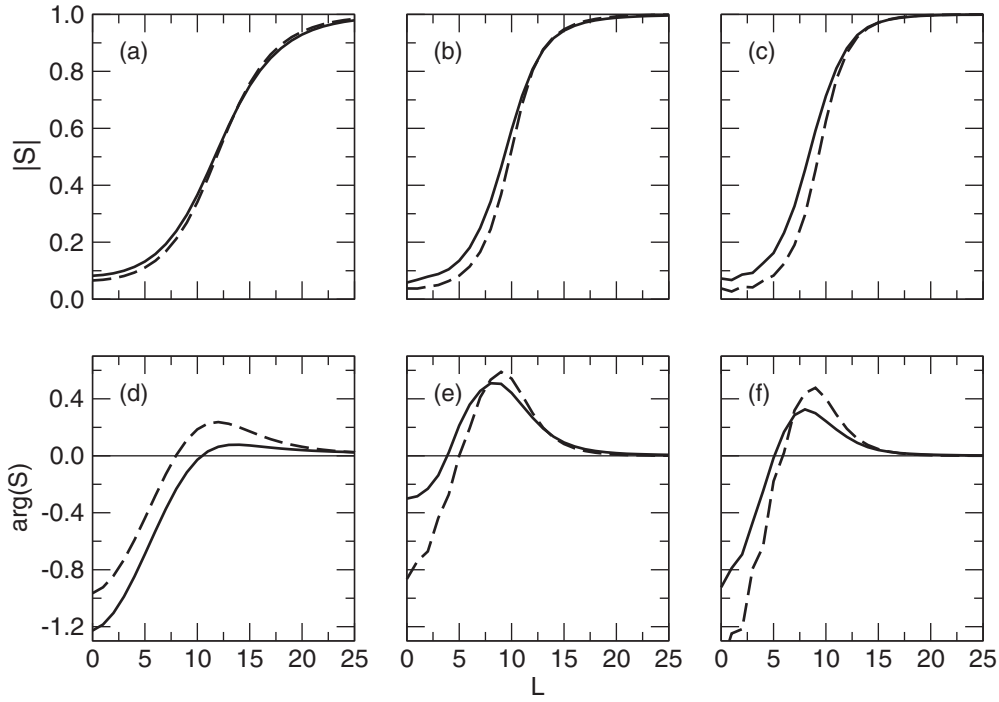

FIG. 2. $|S_L|$ (above) and arg S_L (below) for CDCC calculations for (a) and (d) ^{8}B on ^{58}Ni at $E_{\rm lab} = 29.26$ MeV, (b) and (e) ^{7}Be on ^{58}Ni at $E_{\rm lab} = 24.12$ MeV, and (c) and (f) ^{6}Li on ^{58}Ni at $E_{\rm lab} = 19.04$ MeV. Solid and dashed curves denote full and no-coupling results, respectively.

to a *reduction* in $\sigma_{\rm R}$ of $\Delta\sigma_{\rm R} = -73.49$ mb. This reduction is not large compared to $\sigma_{\rm R}$ without BU coupling, since the WW effect has low $2L + 1$ weight. The WW effect for ^{6}Li is much the same at the higher energy of 24.6 MeV, and is shown here in Fig. 3 which differs from the barrier case of Ref. [12] only insofar as $|S_L|$ is so small for $L \leqslant 2$ that the effect is not very apparent for those values. The corresponding $\Delta\sigma_{\rm R} = -67.7$ mb, comparable to the value near the barrier given in Table I. Figure 4 shows the corresponding increase in differential cross section at backward angles. This is very similar to that in Fig. 1 except that the 5.56 MeV increase in energy has resulted in an almost two orders of magnitude decrease in the differential cross section near 180°.

The above considerations cast the ^{8}B anomaly in a different light since the small effect on the angular distribution coexists with a relatively large effect on $\sigma_{\rm R}$. It is for the ^{8}B case that the RW dominates, especially for the higher L values. One conclusion from all this is that the effect of BU coupling on the differential cross section is quite a different measure of the effect of BU than its effect on the $\sigma_{\rm R}$. For ^{7}Be and ^{6}Li the effects of BU coupling on the angular distributions are visually the same, but the effects on $\sigma_{\rm R}$ are opposite.

In view of this, one may reformulate the ^{8}B anomaly: (i) Why does the BU of ^{8}B lead to such a different balance of WW/RW as a function of L compared with both ^{6}Li and ^{7}Be, noting that the difference between the latter two cases can be understood in terms of the long-range Coulomb BU affecting ^{7}Be but not ^{6}Li? (ii) Why is the case (i.e., of ^{8}B) with the smallest visible change in differential cross section also the case with the largest $\Delta\sigma_{\rm R}$ and $\sigma_{\rm BU}$?

An additional question is, why do the angular distributions for ^{7}Be and ^{6}Li change with BU coupling in such similar ways yet have such different changes in $\sigma_{\rm R}$? Part of the answer is that Coulomb dipole BU does not act upon ^{6}Li at large distances, as can be seen from close inspection of the large-L behavior in Fig. 2. Evidently, the large-L behavior of $|S_L|$ has a small effect on the angular distribution at backward angles. As noted above, this reflects on the use of elastic differential cross section to determine the $\sigma_{\rm R}$. In this connection it can be shown that one can modify arg S_L , without modifying $|S_L|$, imposing Fraunhofer-like oscillations on the angular distribution with zero effect on $\sigma_{\rm R}$.

We now suggest an explanation for WW behavior in these cases. In general $|S_L|$ becomes very small at low L for strongly absorbed particles, but in the present cases near the Coulomb barrier the repulsive Coulomb force evidently reflects the projectiles from the absorptive region. The WW behavior may be an enhancement of this effect, as follows: The overall wave function is a product of terms describing the internal state of the projectile and the motion of the projectile. The interaction with the target nucleus generates a component corresponding to an excited state of internal motion for which the motional factor corresponds to reduced kinetic energy. The excited state amplitude therefore does not extend as far into the absorptive region of the propagating potential as the elastic amplitude, resulting in a reduction in absorption. To the extent that the coupling returns the projectile back to the ground state, there is reduced absorption from the elastic channel. This process, in which some amplitude of the elastic channel wave function is excited, repelled, and then returned to the elastic channel, contributes an intrinsically non-local component to

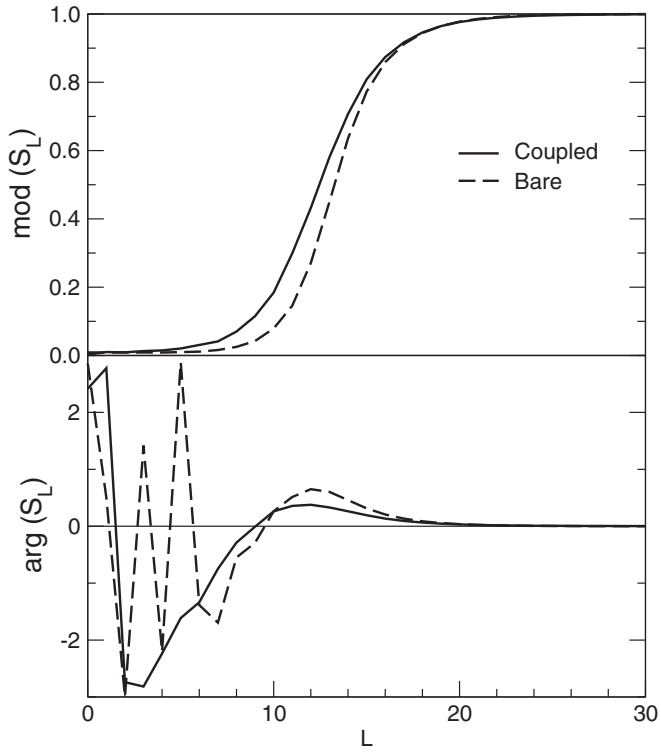

FIG. 3. For 24.6 MeV ^{6}Li on ^{58}Ni, the solid and dashed curves present S_L with and without breakup coupling with, respectively, $|S_L|$ above and arg S_L below. The 2π discontinuity in arg S_L reflects the principal value of arctan.

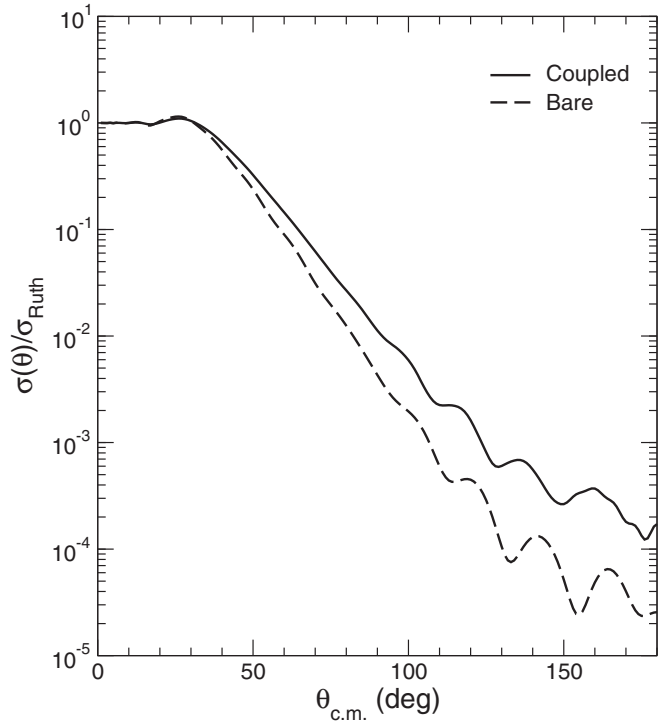

FIG. 4. For 24.6 MeV ^{6}Li on ^{58}Ni, the dashed line is the angular distribution without breakup coupling and the solid line is the angular distribution with breakup coupling.

the effective potential. The probable direct connection with the reduced WW effect for ^{8}B follows since the low breakup threshold for this nucleus may imply a low probability of return to the elastic channel. The consequent reduced change in $|S_L|$ may then be related to the smaller change in the elastic scattering angular distribution for this case while σ_R would be large as a consequence of large breakup cross section extending to high partial waves. From Fig. 5, adapted from Fig. 3 of Ref. [12], it can be seen that the breakup-induced dynamic polarization potential, DPP, for ^{8}B is repulsive for all $r <$ 14 fm, and we shall comment in Sec. II B, in connection with ^{6}He scattering, how the changes in the real potential modify $|S_L|$. The very large repulsive DPP for ^{7}Be for $r < 9$ fm might well be an expression of the effect mentioned above: reduction in absorption through repulsion from the absorptive region.

Very recently, it has been found [16] that the particular WW/RW pattern found for ^{8}B scattering from ^{58}Ni near the Coulomb barrier occurs also for ^{8}B scattering from ^{208}Pb at much higher energies. The underlying mechanism presented there follows the lines proposed above for the barrier energy case.

B. WW effect for ^{6}He on ^{208}Pb at near-barrier energies

Reference [17] presents DPPs arising from projectile breakup for ^{6}He scattering from ^{208}Pb at 22, 27, and 32 MeV and draws attention to a conspicuous WW effect, although it was not called that. At each energy, the DPP has a very long tail that is both attractive and absorptive. Both components reverse sign: the real part is repulsive for $r < 14$ fm, and the imaginary DPP is emissive for $r < 12$ fm, although the total imaginary potential never becomes emissive. Notch tests show that scattering is sensitive to the radial range where the reversal in sign of the DPP occurs, at least for the real part. The WW effect evidently results from the effect of the repulsive DPP reducing the penetration into the strongly absorbing region. This might be connected with the fact that a real notch in this region principally modifies $|S_L|$ and an imaginary notch modifies just arg S_L . This is the opposite of what happens for nucleon scattering or, for the present case, for notches in the region of the tail of the potential.

At both 22 and 32 MeV, the transition from RW for high L to WW for low L occurs for L just above the point where $|S_L| = \frac{1}{2}$. The qualitative change with L in the behavior of $|S_L|$ is very like that noted in Sec. II A in connection with ^{8}B, so this might be characteristic of halo nuclei. The $2L + 1$ weighting ensures that in spite of the conspicuous WW for low L, the net effect of the BU coupling is an increase in σ_R, the change being $\Delta\sigma_R$ = 384.9, 390.8, and 404.9 mb for 22, 27, and 32 MeV, respectively. The factor $(Z_2A_1 - A_2Z_1)/(A_1A_2)$ is 0.5 in this case, larger than for the cases studied in Ref. [12]. Interestingly, the increase in $\Delta\sigma_R$ does not hold for calculations which include only the coupling to the 2^+ resonance in ^{6}He. For each energy, the 2^+ excitation generates a WW effect for the lower values of L but does not generate a graphically conspicuous RW effect for higher L. As a result, coupling to the 2^+ resonance results in a *reduction* in the reaction CS, with $\Delta\sigma_R = -11.8, -14.3,$ and -11.4 mb for the same three energies. This can be interpreted as a result

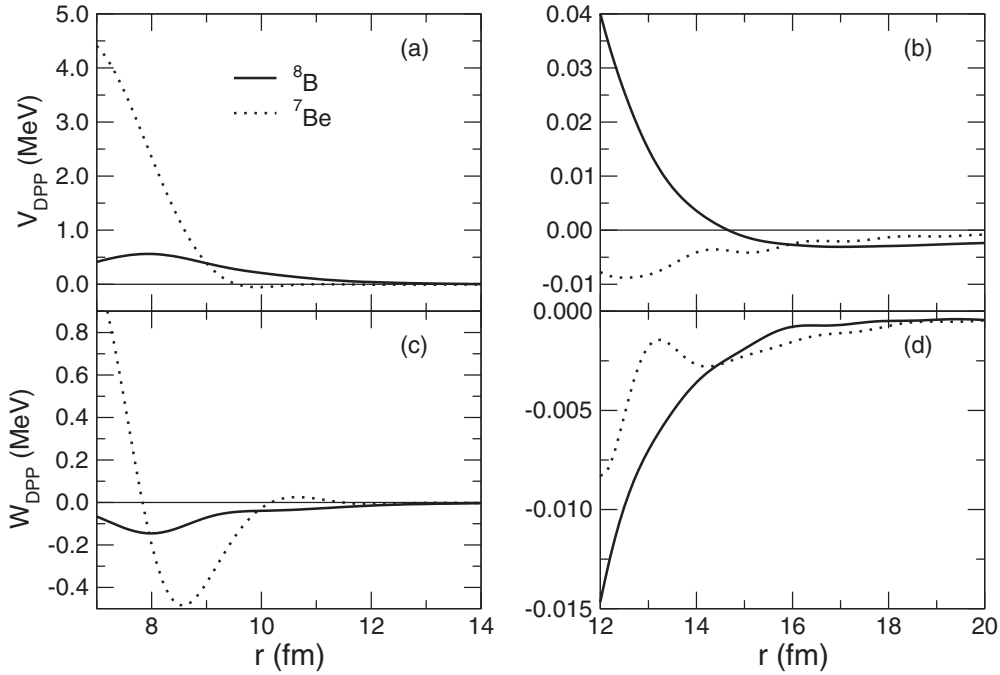

FIG. 5. DPPs due to breakup coupling for ^{8}B(solid curves) and ^{7}Be (dotted curves). The real parts are shown in (a) and (b); the imaginary parts, in (c) and (d). Panels (b) and (d) present the DPPs for the outer region on an expanded scale.

of the excited amplitude of the projectile having less energy and therefore less tunneling probability. The de-excitation of the 2^+ state returns it to the elastic channel in accord with Austern's account [18] of non-locality.

III. MORE GENERAL EXAMPLES OF WW

The effect is generally less marked for lighter ions and for higher energies, and some regularities emerge from the cases presented here. The effect found for deuteron scattering might be of consequence for the extraction of spectroscopic information from deuteron-induced reactions.

A. WW effect for deuteron scattering

The WW effect occurs in calculations of the contribution of deuteron breakup to the deuteron-nucleus interaction. For deuterons of 56, 79, and 120 MeV on ^{58}Ni, Ref. [1] drew attention to the fact that $|S_L|$ increased for certain L values and energies. The magnitude of the WW effect was largest for 56 MeV deuterons, and was almost absent at 120 MeV (but present to a small degree when there was only S-wave breakup.) The DPP arising from breakup had a region of emissivity around 4 fm. This emissivity was strongly correlated with the occurrence of the WW effect. At all energies the DPP was also emissive at the nuclear center.

There was a tendency, like that seen in Table I, for the actual breakup cross section $\sigma_{\rm BU}$ to exceed $\Delta\sigma_{\rm R}$, the increase in the reaction CS due to BU coupling. However, there was an anti-correlation between this tendency and the degree of WW effect and there was no such excess at the lowest energy, where both WW and emissivity were most apparent. The increase in WW with decreasing deuteron energy might be of concern since much spectroscopic information from (d,p) reactions has been extracted at quite low energies.

B. WW effect for ^{6}Li BU at higher energies.

The DPPs due to projectile breakup were studied [19] for ^{6}Li on ^{12}C at 90, 123, 168, 210, and 318 MeV. As was the case for deuteron scattering, WW was seen more consistently for S-wave BU (SBU) than for S+D-wave BU (SDBU). WW was clearly present for both SBU and SDBU at 90 MeV, almost doubling $|S_L|$ for $L = 13$ with SDBU, but was not present at the higher energies, although there was a bump approaching WW at 123 MeV, see Fig. 9 of Ref. [19]. For SBU, however, WW was still present, but only just, at 210 MeV, but there was no WW for 318 MeV. This energy dependence also occurs for deuteron BU, suggesting generic behavior. We have seen that for all cases in Table I, as well as the deuteron cases, $\sigma_{\rm BU}$ exceeded $\Delta\sigma_{\rm R}$; this is true for ^{6}Li too, by a factor of about 3 at 90 MeV and about 2 at 318 MeV. The WW effect is most apparent at the lowest energy, as it was for deuterons.

C. WW effect for ^{6}He on ^{208}Pb at 66 MeV

Prior to the calculations reported in Sec. II B, similar calculations had been performed [20] at a range of higher energies up to 66 MeV and consistent DPPs were found over the whole energy range. The ^{6}He wave functions were less realistic than those for the calculations reported in Sec. II B, and the DPPs and changes in S_L were somewhat too large to a degree that can be judged from Ref. [17]. Nevertheless, the calculations [20] clearly show that coupling to BU channels

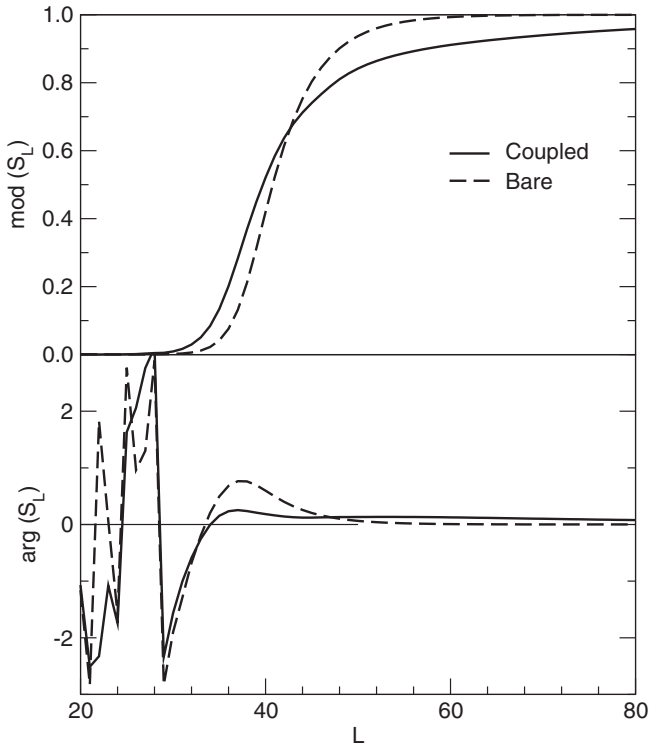

FIG. 6. For 66 MeV ^{6}He on ^{208}Pb, the solid and dashed curves present S_L with and without breakup coupling with, respectively, $|S_L|$ above and arg S_L below.

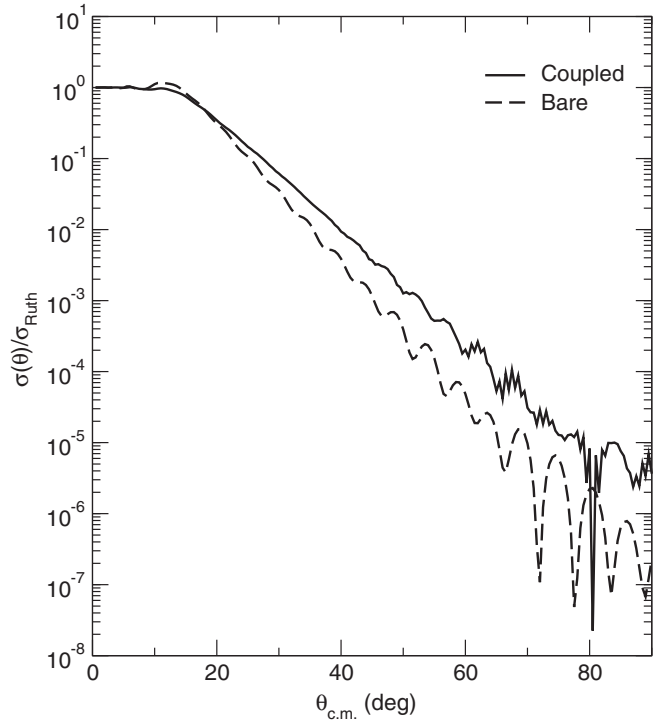

FIG. 7. For 66 MeV ^{6}He on ^{208}Pb, the dashed line is the angular distribution without breakup coupling and the solid line is the angular distribution with breakup coupling.

results in marked WW for 66 MeV ^{6}He scattering from ^{208}Pb at energies far above the Coulomb barrier. Figure 6 presents the effect of the coupling on the S matrix. It can be seen that for $L \geqslant 45$ and continuing to the highest L, $|S_L|$ is greatly reduced as a result of the breakup, i.e., it changes the "right way." As a result, the reaction cross section is increased by the BU coupling from 3558.5 to 5448.3 mb. It can also be seen that arg S_L increases from about the same value of L upward, corresponding to the strong attractive tail of the DPP [20]. The reduction of arg S_L for lower L corresponds, as shown explicitly by $S_L \rightarrow V(r)$ inversion [20], to repulsion for $r < 15$ fm. Reference [20] also shows the imaginary DPP becoming emissive for $r < 13$ fm, and this might be associated with the conspicuous WW effect in which $|S_L|$ substantially increases for all L below about 45, at least those for which it is visible on the graph. The corresponding changes in angular distribution are shown in Fig. 7.

For 66 MeV ^{6}He, the explanation of why the excitation of the projectile leads to a reduction in absorption, along with a repulsive change in the real potential, may be somewhat different from what appeared to apply at energies near the barrier. The excitation appears to deflect the path of the six projectile nucleons away from the nucleus in the surface where there are strong gradients for both the real and imaginary parts of the propagating interaction potential so that the projectile "feels" less attraction and absorption before it de-excites to ^{6}He. Such processes cannot be represented through a local density model.

D. WW effect, or its absence, due to coupling of pickup channels: Cases of ^{3}He, deuteron, and proton scattering

Coupled reaction channel (CRC) calculations [21] in which ^{4}He channels were coupled to ^{3}He elastic scattering for $E(^{3}\text{He}) = 37$ and 51 MeV reveal some degree of WW in the behavior of $|S_L|$ for values of L near the point (the "kink") where $|S_L|$ begins to increase rapidly with L. Unlike the cases where weakly bound and halo light nuclei interact with heavier nuclei at near barrier energies, but like the deuteron and ^{6}Li breakup cases at higher energies, there is no WW effect at the lowest L values.

For 52 MeV deuterons scattering on ^{40}Ca [22], CRC calculations of pickup and stripping contributions revealed an effect on $|S_L|$ that is generally RW, but with a small number of WW L values near the kink in $|S_L|$.

There is no WW effect of pickup coupling for 25 or 61.3 MeV protons on ^{8}He, nor with pickup coupling for proton scattering on ^{10}B reported in Ref. [23]. This is also the case for pickup (deuteron channel) coupling for 30.3 MeV protons on ^{40}Ca, see Ref. [24].

These results together suggest that the WW effect is most evident when the absorption in the coupled reaction channel is relatively great.

E. WW and its interpretation in inelastic scattering of ^{16}O from ^{12}C

For 192 MeV ^{16}O scattering from ^{12}C, rotational excitations of ^{12}C led to a substantial WW effect that was associated with a strongly emissive DPP [25]. The WW effect was present only

when the imaginary part (as well as the real part) of the optical potential was deformed to generate the rotational excitations. Calculations were presented suggesting that a strong repulsive DPP keeps the interacting nuclei from the radial range in which absorption occurs. This needs further exploration, but it resembles the WW effect in the ^{6}Li, ^{7}Be, and ^{8}B cases.

IV. SUMMARY AND CONCLUSIONS

We have drawn attention to a counter-intuitive response of $|S_L|$, the modulus of the elastic scattering S matrix, in many cases when collective, reaction, or breakup states are coupled to the elastic channel. In such cases the coupling leads to an increase in $|S_L|$ for particular partial waves, leading to a reduction in the corresponding partial reaction cross-sections $(\pi/k^2)(2L+1)(1-|S_L|^2)$. This may occur when spin is included and $|S_{LJ}|$ rather than $|S_L|$ increases. The effect can be very marked, as in Figs. 2, 3, and 6. In other cases the effect is small, occurring for a restricted number of number of partial waves and may disappear at higher energies. However, we have very recently shown that the pattern of increase and decrease in $|S_L|$ that applies for ^{8}B scattering near the Coulomb barrier occurs also at much higher energies [16]. In that particular case we have suggested a mechanism for the increase in $|S_L|$, but the nature of the effect over the range of cases remains obscure.

Although our discussion has mostly related to $|S_L|$, we have included arg S_L in the figures. This quantity is informative concerning the response of the real potential to channel coupling, particularly in the surface regions, and is referred to explicitly in the ^{6}He cases. The ultimate account of the effects described here will doubtless include an account of the origin of the pattern of attraction and repulsion induced by channel coupling.

The occurrence of WW has a bearing on general questions concerning elastic scattering, such as, why, in particular cases, does breakup coupling have a (relatively) small effect on elastic scattering angular distributions and yet have a (relatively) large reaction CS? The non-local effects that are implicated make the application to direct reactions of optical potentials, which are fitted to elastic scattering data, problematic. It is not sufficient to correct for the Perey effect [26] and wrong to assume that all non-locality is similar in effect to that associated with Perey-Buck [27], in effect, to knock-on exchange. As mentioned in the Introduction, the non-locality discussed here is not related to the Perey-Buck form; reaction channel coupling can even lead to an "anti-Perey" effect [28].

The effect that we have surveyed in this paper needs to be understood before a rigorous extraction of spectroscopic information from direct reactions can be ensured. For example, it is generally supposed that the (d,p) stripping peak leads to good values of the spectroscopic factor even when the rest of the transfer angular distribution is not fitted. This must be regarded as an unsafe assumption while there is evidently so much that is not understood regarding the interaction of deuterons with nuclei. At typical stripping experiment energies, deuteron breakup leads to a strong WW effect [1] with an associated emissive region in the DPP, strongly suggestive of non-local effects. It is well-known that local representations of non-locality modify the wave function and, in the case of dynamical rather than exchange non-locality, in a way immune to standard Perey-effect correction. A manifestation of the non-locality of the underlying DPP that arises with pickup coupling was discussed in Ref. [29].

In this paper we have not given a general explanation of the WW effect covering all cases, but we have related various instances of it to different characteristics of the reactions. For example, the fact that the effect is less marked for ^{8}B than it is for ^{7}Be and ^{6}Li is related to the apparently anomalous relation between the magnitude of $\sigma_{\rm BU}$ and the effect on the elastic scattering angular distribution [16]. A prime influence on whether there is a WW effect is the strength of the absorption in the coupled channels or in the non-diagonal coupling potentials.

The WW effect is evident when specific reaction, inelastic, or breakup channels are explicitly coupled to the elastic channel. However, these processes are also operative in elastic scattering when channel coupling is not calculated explicitly. They contribute to what is customarily represented as a local and L-independent phenomenological OMP. When data are fitted with the CC calculations, the bare potentials are, ideally at least, adjusted to give what is often an improved fit to the elastic scattering data. The customary phenomenological OMP is a local and L-independent substitute for a highly non-local and probably L-dependent potential. Ideally, this should be accounted for in the analysis of nuclear reactions. We re-emphasize that the non-locality involved is not just that of the Perey-Buck kind, and the probable L dependence [30] is distinct from the parity dependence associated with certain exchange processes, particularly those involving light nuclei.

ACKNOWLEDGMENTS

I am very grateful to N. Keeley for many insightful discussions and some crucial calculations and for producing publishable figures.

[1] R. S. Mackintosh and D. Y. Pang, Phys. Rev. C **86**, 047602 (2012).
[2] H. Feshbach, Ann. Phys. (NY) **5**, 357 (1958); **19**, 287 (1962).
[3] C. L. Rao, M. Reeves, and G. R. Satchler, Nucl. Phys. A **207**, 182 (1973).
[4] C. A. Coulter and G. R. Satchler, Nucl. Phys. A **293**, 269 (1977).
[5] G. H. Rawitscher, Nucl. Phys. A **475**, 519 (1987).
[6] D. F. Jackson and R. C. Johnson, Phys. Lett. B **49**, 249 (1974).
[7] S. J. Freeman and J. P. Schiffer, arXiv:1207.4290.
[8] F. Flavigny *et al.*, Phys. Rev. Lett. **110**, 122503 (2013).
[9] K. L. Jones, Phys. Scr. T **152**, 014020 (2013).
[10] R. S. Mackintosh and A. A. Ioannides, in *Advanced Methods in the Evaluation of Nuclear Scattering Data*, Lecture Notes in Physics Vol. 236, edited by H. J. Krappe and R. Lipperheide (Springer-Verlag, New York, 1985), p. 283.
[11] E. F. Aguilera *et al.*, Phys. Rev. C **79**, 021601(R) (2009).

[12] N. Keeley, R. S. Mackintosh, and C. Beck, Nucl. Phys. A **834**, 792c (2010); this paper has misprints: on the first text line of page 794c it says "decrease" where it means "increase," and vice versa.
[13] N. Keeley, paper presented at the 10th International Conference on Nucleus-Nucleus Collisions, August 16–21, 2009, Beijing (unpublished)
[14] B. Buck and A. A. Pilt, Nucl. Phys. A **280**, 133 (1977).
[15] P. Mohr, Phys. Rev. C **87**, 035802 (2013).
[16] R. S. Mackintosh and D. Y. Pang, Phys. Rev. C **88**, 014608 (2013).
[17] R. S. Mackintosh and N. Keeley, Phys. Rev. C **79**, 014611 (2009).
[18] N. Austern, Phys. Rev. B **137**, 752 (1965).
[19] D. Y. Pang and R. S. Mackintosh, Phys. Rev. C **84**, 064611 (2011).
[20] N. Keeley and R. S. Mackintosh, Phys. Rev. C **71**, 057601 (2005).
[21] N. Keeley and R. S. Mackintosh (unpublished).
[22] N. Keeley and R. S. Mackintosh, Phys. Rev. C **77**, 054603 (2008).
[23] R. S. Mackintosh and N. Keeley, Phys. Rev. C **76**, 024601 (2007).
[24] R. S. Mackintosh and N. Keeley, Phys. Rev. C **85**, 064603 (2012).
[25] R. S. Mackintosh and S. G. Cooper, Nucl. Phys. A **494**, 123 (1989).
[26] F. G. Perey, in *Direct Interactions and Nuclear Reaction Mechanisms*, edited by E. Clemental and C. Villi (Gordon and Breach, New York, 1963), p. 125.
[27] F. G. Perey and B. Buck, Nucl. Phys. **32**, 353 (1962).
[28] S. G. Cooper and R. S. Mackintosh, Nucl. Phys. A **511**, 29 (1990).
[29] R. S. Mackintosh and N. Keeley, Phys. Rev. C **81**, 034612 (2010).
[30] R. S. Mackintosh, arXiv:1302.1097 (2013).